Open Access

Biogeosciences
Discussions

Observed increase in springtime surface partial pressure of CO_2 in the east equatorial Indian Ocean during 1962–2012

L. Xue, W. Yu, H. Wang, L. Feng, Q. Wei, and C. Ning

First Institute of Oceanography, State Oceanic Administration, Qingdao 266061, China

Correspondence to: L. Xue (xueliang@fio.org.cn)

BGD

11, 521–549, 2014

Observed pCO_2 increase in the equatorial Indian Ocean

L. Xue et al.

Title Page

Abstract	Introduction
Conclusions	References
Tables	Figures

Back | Close

Full Screen / Esc

Printer-friendly Version

Interactive Discussion

Abstract

Rapidly rising atmospheric CO_2 and global warming may have been impacting the ocean, and, in contrast, the response of surface CO_2 partial pressure (pCO_2) in the equatorial Indian Ocean is poorly understood. In this study, we attempted to evaluate the variation of springtime sea surface pCO_2 in the east equatorial Indian Ocean (5° N to 5° S along 90° E and 95° E, EIO), which is relatively better occupied, using data collected in May 2012, together with the historical data since 1962 (LDEO_Database_V2012). Results showed that sea surface pCO_2 in the investigation area increased from $\sim 308\,\mu atm$ in April 1963, through $\sim 373\,\mu atm$ in May 1999, to $\sim 387\,\mu atm$ in May 2012, with a mean increase rate of $\sim 1.7\,\mu atm\,yr^{-1}$. Given that the EIO during the study period was almost always a CO_2 source to the atmosphere, it was obvious that the observed increase of sea surface pCO_2 with time in this region was not due to the local uptake of CO_2 via air–sea exchange, although quickly increasing atmospheric CO_2 had the potential to increase seawater pCO_2. Further, we checked the effects of variations in sea surface temperature, salinity, mixed layer depth and chlorophyll a (as a proxy of biological production) on surface pCO_2. We found surface ocean warming partially contributed to sea surface pCO_2 increase, whereas the effects of salinity, mixed layer depth, and biological activity were not significant. The pCO_2 increase in the equatorial waters (CO_2 source to the atmosphere) was probably due to the transport of carbon accumulated in the CO_2 sink region (to the atmosphere) towards the CO_2 source region on a basin scale via ocean circulation. Additionally, our study showed that more and more release of CO_2 from the ocean to the atmosphere and big pH reduction (0.07 pH units) in the past 50 yr (from 1963 to 2012) may have occurred in the EIO. It also demonstrated that ocean acidification may have taken place in the global ocean, not just limited to the CO_2 sink region.

Observed pCO_2 increase in the equatorial Indian Ocean

L. Xue et al.

1   Introduction

Atmospheric carbon dioxide (CO_2) levels have risen from ~ 280 ppm (parts per million in volume) in the pre-industrial revolution ear to a 2012 value of ~ 393 ppm (Tans and Keeling, 2013) due to quickly increasing human activities, which might have caused

5   global climate change (Denman et al., 2007). Meanwhile, the ocean as a CO_2 sink to the atmosphere plays a key role in alleviating the increase of CO_2 in the atmosphere (Sabine et al., 2004; Takahashi et al., 2009), absorbing roughly half of anthropogenic CO_2 from fossil fuel burning and cement production (Sabine et al., 2004). Ocean CO_2 uptake, however, is not benign. As we know that the uptake of anthropogenic CO_2 by

10   the ocean will raise CO_2 concentrations in seawater, hence lower pH and $CaCO_3$ saturation state, and change speciation of carbonate chemistry (i.e., ocean acidification, OA) via a series of chemical reactions when CO_2 was dissolved into seawater (Millero, 2007). Furthermore, OA will induce negative feedbacks on oceanic CO_2 uptake and even significant impacts on marine organisms (especially for calcifying organisms) and

15   ecosystems (Doney et al., 2009).

Sea surface partial pressure of CO_2 (pCO_2) is primarily determined by temperature, salinity, dissolved inorganic carbon (DIC) and total alkalinity (TA) (Millero, 2007), and to a large extent could directly reflect the change in seawater CO_2 concentration (e.g., Xue et al., 2012) and even the status of OA. Furthermore, sea surface pCO_2 data is

20   relatively easy to obtain (e.g., via underway measurements on the volunteer observing ships) and a large number of data have been accumulated since 1960s (Sabine et al., 2013). Thus, sea surface pCO_2 is often used for characterizing the capability of the ocean to absorb atmospheric CO_2, and for monitoring the change in seawater CO_2 concentration and the response of sea surface pCO_2 to rapidly increasing atmospheric

25   CO_2. During recent years, more attention has been therefore paid to studies on the oceanic pCO_2 change. For example, long-term increases in seawater CO_2 levels have been observed in a variety of oceanic zones such as subtropical North Pacific and North Atlantic (Bates, 2007; Lenton et al., 2012), the equatorial Pacific (Takahashi et al.,

2006), subarctic North Pacific and North Atlantic (Omar and Olsen, 2006; Lenton et al., 2012) and the Southern Ocean (Lenton et al., 2012).

In the Indian Ocean, a lot of CO_2 related studies such as carbonate parameter distributions and related controlling processes as well as its role in the global carbon cycle were conducted primarily propelled by several national or international programs such as JGOFS (Joint Global Ocean Flux Study) and WOCE (World Ocean Circulation Experiment) (e.g., Naqvi, 2002). For instance, Sabine et al. (2002) found that the DIC and TA distributions in the Indian Ocean were dominated by the large-scale circulation patterns and the strength of the biological pump. Bates et al. (2006) examined the spatial and temporal variability of upper ocean carbonate parameters and air–sea CO_2 exchange in the Indian Ocean, and pointed out that the Arabian Sea, Bay of Bengal, and the equatorial belt ($10°$ N–$10°$ S) were perennial sources of CO_2 to the atmosphere. Sardessai et al. (2010) found the northeastern Indian Ocean showed significant intraseasonal variability in CO_2 fluxes, acting as a strong sink of CO_2 during southwest monsoon, a weal sink during fall intermonsoon and a weak source during winter monsoon.

In contrast, studies on the variation of the Indian Ocean surface water pCO_2 are relatively sporadic due to lack of enough pCO_2 measurements (Takahashi et al., 2009; Lenton et al., 2012; Sabine et al., 2013; Sarma et al., 2013). For example, Metzl (2009) for the first time investigated the decadal variability of the CO_2 fugacity (fCO_2, a parameter very close to pCO_2 in meaning and magnitude) at the sea surface in the southwestern Indian Ocean (a CO_2 sink) and corresponding Antarctic sector, and observed that oceanic fCO_2 increased at a rate of $2.11 \pm 0.07 \, \mu atm \, yr^{-1}$ during 1991–2007. In addition, related studies based on models were also conducted in the Indian Ocean. For instance, it was reported that the Arabian Sea and Southern Peninsular India interannual CO_2 emission anomalies were related to the Indian Ocean Dipole (IOD) and the El Niño-Southern Oscillation (ENSO) (Valsala and Maksyutov, 2013). A more recent study using the ocean biogeochemical models suggested a small enhancement in the CO_2 sink over the period 1990–2009 in the southern Indian Ocean (Sarma et al.,

2013), which is not consistent with the observations in the southwestern Indian Ocean by Metzl (2009). Therefore, more studies based on in-situ observations are needed to confirm the model results.

Significant increases in sea surface pCO_2 in the equatorial Pacific have been in-dicated (Feely et al., 1999; Takahashi et al., 2003; Ishii et al., 2009). The equatorial Indian Ocean is different from the Pacific in a number of ways. For instance, the Indian Ocean lacks steady equatorial easterlies and hence there is no climatic equatorial up-welling in the eastern part (Schott et al., 2009). As a result, the east equatorial Indian Ocean (EIO) does not have a significant source of CO_2 as in the eastern tropical Pa-cific (Takahashi et al., 2009). However, under the forcing of rising atmospheric CO_2 and global warming, the response of surface pCO_2 in the EIO, which serves as a perennial CO_2 source to the atmosphere (Bates et al., 2006; Takahashi et al., 2009), is poorly understood.

In this paper, we attempt to check the variability of springtime surface pCO_2 in the EIO (Fig. 1), which is relatively better occupied, using data collected during May 2012, together with the historical data since 1962 integrated by Takahashi et al. (2013) (i.e., LDEO_Database_V2012), and to explore the possible factors responsible for it by an-alyzing the effects of temperature, salinity, mixed layer depth (MLD), biological produc-tion and ocean circulation. At last, the potential influences of oceanic pCO_2 increase were simply discussed.

2 Material and methods

2.1 Study site

The study site was located in the EIO, extending from 5° N to 5° S along 90° E and 95° E (Fig. 1). The wind field in the equatorial Indian Ocean is unique relative to the Pacific and Atlantic, with weak and westerly annual mean, and strong semiannual an-nual cycle. Consequently, the equatorial currents are quite different in features from

Title Page

Abstract | Introduction

Conclusions | References

Tables | Figures

◄ | ►

◄ | ►

Back | Close

Full Screen / Esc

Printer-friendly Version

Interactive Discussion

those in the other oceans (Schott and McCreary, 2001). The surface currents in the equatorial Indian Ocean reverse directions seasonally, with a weak westward flow during winter and summer, and a strong eastward flow during the intermonsoon periods in spring (April/May) and fall (October/November) (Schott and McCreary, 2001). The strong eastward currents are now widely known as Wyrtki jets (Wyrtki, 1973; Schott and McCreary, 2001). Another important current in the equatorial Indian Ocean is the transient Equatorial Undercurrent (Knauss and Taft, 1964). It exists only during part of the year due to lack of sustained easterlies, typically February–June with an easterly component.

2.2 Data sources

Sea surface pCO_2 data in the MOMSEI cruise (Monsoon Onset Monitoring and its Social and Ecosystem Impact) were collected during 1–9 May 2012. Sea surface pCO_2 was continuously measured every 15 min with a HydroC™ CONTROS sensor. More details on pCO_2 measurements were described by Saderne et al. (2013). In brief, the CO_2 mole fraction in a headspace behind a membrane equilibrator is measured using a two-wavelength non-dispersive infra-red detector (NDIR). The equilibrator consists of a flat silicone composite membrane, the NDIR unit and additional sensors for pressure, temperature and relative humidity measurements. These additional sensors are used for correcting the NDIR signal and calculating the partial pressure. In addition, regular zeroings are automatically performed to correct the drifting of the instrument with time by scrubbing CO_2 from the internal gas stream. An overall accuracy is estimated better than ±1 % of the upper range value (Saderne et al., 2013). At the meanwhile, during the MOMSEI cruise sea surface temperature (SST) and salinity (SSS) were collected every 15 min using a SBE 21 Seacat Thermosalinograph.

The historical data before 2012 were integrated by Takahashi et al. (2013) (i.e., LDEO_Database_V2012) (Tables 1 and 2). The Takahashi LDEO database of direct global pCO_2 at the surface are based on measurements made using air–seawater equilibration methods (Takahashi et al., 2013). Good quality control for all data points

have been examined individually as they were integrated into this database. The uncertainty of the pCO$_2$ data is estimated about ±2.5 µatm on the average, given differences in equilibrator designs, calibration methods and some interpolated parameters (Takahashi et al., 2013).

Atmospheric CO$_2$ data in this study are from monthly average values measured as the mole fraction in dry air on Mauna Loa, Hawaii (Table 2), where the longest direct measurement of atmospheric CO$_2$ is recorded. The atmospheric pCO$_2$ were corrected to 100 % humidity at the mean SST (29.60 ∘C) and SSS (34.16) during the investigation period, following Jiang et al. (2008). In addition, several ancillary parameters such as SST, MLD and chlorophyll a (Chl a) (Table 2) were used.

3 Results and discussion

3.1 Change in surface pCO$_2$ since 1962

Figures 2 and 3 show all the pCO$_2$ data collected since 1962 in the EIO. Spatially, pCO$_2$ distributions are relatively homogeneous in each cruise, with standard deviation less than 9 µatm (Fig. 2 and Table 1). Latitudinally, sea surface pCO$_2$ showed some common features (Fig. 3). For instance, high pCO$_2$ values with large variability on a small regional scale were observed between 0° N and 3° N in 1963, 2007 and 2012, and surface pCO$_2$ decreased towards the south from around 2° S in 1963, 1995, 1999 and 2012, probably associated with temperature (Fig. 3). In addition, high pCO$_2$ values in 1995 and 1999 were found in the southwestern part of the study area (Figs. 2 and 3), possibly due to high salinity (Fig. 3).

Temporally, gradual increase in sea surface pCO$_2$ with time was the most evident feature (Figs. 2–4, Table 1), although an exception occurred in July 1987. Sea surface pCO$_2$ in July 1987 was similar to, or larger than that in February 1995, probably due to high salinity in the eastern part of the study area in July 1987 (Figs. 2 and 3). Generally, the mean value of sea surface pCO$_2$ in the investigation area in-

creased from $\sim 308\,\mu$atm in April 1963, through $\sim 373\,\mu$atm in May 1999, to $\sim 387\,\mu$atm in May 2012 (Fig. 4a and Table 1). If data from all cruises during 1962–2012 were considered, sea surface pCO_2 would have an increase rate of $1.70\,\mu$atm yr^{-1} (Fig. 4). Considering that not all the cruises were conducted in the same season and areas, we checked the pCO_2 variation using data collected at Location A, B, and C (these data were almost collected during the same season (April/May) and at the same location, Fig. 1), which removes the possible bias due to spatial and temporal variability. Results showed that from 1963 to 2012 during spring (April/May), sea surface pCO_2 had a mean increase rate of $\sim 1.75\,\mu$atm yr^{-1} (Fig. 4). Also we compared the surface pCO_2 between April 1963 and May 2012 along the equator from 89.5° E to 94.5° E, and found during the past 50 yr since the International Indian Ocean Expedition (IIOE, from 1960–1965), surface pCO_2 increased from $307 \pm 4\,\mu$atm in April 1963 to $392 \pm 6\,\mu$atm in May 2012 (Fig. 4), with a mean rate of $1.70\,\mu$atm yr^{-1}. The increase rate of surface pCO_2, $\sim 1.7\,\mu$atm yr^{-1}, obtained using all data measured during 1962–2012, and data just from fixed points (Location A, B and C) as well as via difference between 1963 and 2012 are almost entirely the same, indicating that this mean increase rate is reasonable and reliable. This pCO_2 increase rate in the EIO is similar to that in the subtropical North Atlantic (Bates, 2007), higher than that in the western tropical North Atlantic (Park and Wanninkhof, 2012), and lower than that in the equatorial Atlantic and Pacific (Oudot et al., 1995; Takahashi et al., 2006) (Table 3).

However, assessing the trend of surface pCO_2 in our study area is challenging due to lack of continuous data. Surface pCO_2 might also be modulated by some climate events such as the ENSO and the IOD. For example, Takahashi et al. (2003) investigated the effects of the Pacific Decadal Oscillation phase shift on decadal pCO_2 variation, and found during the decade before the shift, surface pCO_2 in the central and western equatorial Pacific reduced at a mean rate of about $-20\,\mu$atm per decade, whereas after the shift, it rised at $\sim 15\,\mu$atm per decade. Also model studies showed that the Arabian Sea and Southern Peninsular India interannual CO_2 emission anomalies were related to the IOD and ENSO (Valsala and Maksyutov, 2013). In our study,

Observed pCO_2 increase in the equatorial Indian Ocean

L. Xue et al.

influence of climate events are not taken into account due to lack of continuous data since 1962. Especially, there were no data available during 1963–1987, and we don't know what happened to sea surface pCO_2 during this period. These may cause uncertainties for the determination of pCO_2 trend. However, these climate signals will fade away when timescales lengthen (Fay and McKinley, 2013). Thus, our study at least provides the mean rate of sea surface pCO_2 increase from 1962 to 2012, which is important for understanding the variation of ocean CO_2 system (carbon speciation) and its potential effects on marine organisms. It also implies that big changes in carbon chemistry (e.g., OA) and even other marine biogeochemical processes may have taken place in the Indian Ocean since the IIOE. Thus, it is very essential to conduct IIOE-2 (planned in 2015–2020) from the viewpoint of global change, besides the fundamental developments in technology.

3.2 Possible factors responsible for sea surface pCO_2 increase

It was obvious that the observed increase of springtime sea surface pCO_2 with time was not due to the local uptake of CO_2 via air–sea exchange, given that the EIO was almost always a CO_2 source to the atmosphere (Fig. 4, Bates et al., 2006; Takahashi et al., 2009). Although atmospheric CO_2 was rapidly rising since 1962, which has the potential to increase seawater pCO_2 via air–sea equilibrium and reduce the CO_2 release from the ocean to the atmosphere, pCO_2 at the sea surface in the EIO was still larger than that in the atmosphere during 1962–2012 (Fig. 4), indicating no local uptake of CO_2 from the atmosphere in the EIO (Bates et al., 2006; Takahashi et al., 2009). Since sea surface pCO_2 was mainly influenced by physical and biological processes such as temperature, horizontal and vertical mixing, advection, ocean circulation, and biological activity (e.g., Sabine and Key, 1998; Xue et al., 2012), we will check the effects of SST, SSS, MLD, ocean circulation and Chl a (as a proxy of biological production) on surface pCO_2 in the following sections.

3.2.1 Influence of SST, SSS, MLD, and Chl *a*

Generally, seawater $p\mathrm{CO}_2$ increases with temperature (e.g., Takahashi et al., 1993). However, we found that sea surface $p\mathrm{CO}_2$ increase in the EO did not correspond to SST rise. For instance, surface $p\mathrm{CO}_2$ in 1987–2012 was much higher than that in July 1962 and April 1963, whereas SST in July 1962 and April 1963 was almost at the same level as that in 1987–2012 (Fig. 5a). This suggests temperature may not be responsible for surface $p\mathrm{CO}_2$ increase during the study period. Further, we checked the trend of SST from 1962 to 2012 using ERSST data (Extended Reconstructed Sea Surface Temperature, Table 2) and found SST significantly increased with an increase rate of $0.013\,°\mathrm{C}\,\mathrm{yr}^{-1}$ (Fig. 6a). That is to say, during this period surface ocean warming occurred. It will cause surface $p\mathrm{CO}_2$ to increase at a rate of $\sim 0.1\,\mu\mathrm{atm}\,\mathrm{yr}^{-1}$ alone based on the $p\mathrm{CO}_2$-temperature relationship (i.e., $(\alpha p\mathrm{CO}_2/\alpha T)/p\mathrm{CO}_2 = 0.0423\,°\mathrm{C}^{-1}$) (Takahashi et al., 1993). This is coherent with the increase rate of $p\mathrm{CO}_2$ normalized to a constant temperature of $29.60\,°\mathrm{C}$ ($np\mathrm{CO}_2$), the mean temperature of all data. We found surface $np\mathrm{CO}_2$ still increased at a mean rate of $1.62\,\mu\mathrm{atm}\,\mathrm{yr}^{-1}$, i.e., the non-temperature effect (Fig. 4b). Thus, surface $p\mathrm{CO}_2$ increase during the period 1962–2012 was partially trigged by surface ocean warming, and was essentially due to change in seawater CO_2 concentration.

In general, surface $p\mathrm{CO}_2$ in the open ocean rises with increased salinity as shown in Figs. 3 and 5. From Fig. 3, we found SSS variation may not be responsible for surface $p\mathrm{CO}_2$ increase. For example, SSS between $2°\mathrm{S}$ and $2°\mathrm{N}$ in May 1999 was almost the same (34.2–34.6) as that in May 2012, but $np\mathrm{CO}_2$ in May 2012 was clearly higher than that in May 1999 (Figs. 3 and 5). Although no significant trend in SSS from Fig. 6b could be found, more recently Subrahmanyam et al. (2011) reported a significant freshening trend in SSS during 2002–2007 in the EIO, which indicates a decrease of surface $p\mathrm{CO}_2$. Thus, we inferred that SSS change may not be the major factor triggering $p\mathrm{CO}_2$ increase.

Observed $p\mathrm{CO}_2$ increase in the equatorial Indian Ocean

L. Xue et al.

MLD deepening will bring CO_2-rich waters to surface layer, leading to high pCO_2 level (e.g., Dumousseaud et al., 2010). We find MLD thickness showed an increase trend during 1969–1985, a decrease trend during 1985–1997 and then an increase trend during 1997–2009 (Fig. 6c). Overall, there is no significant trend for MLD during 1969–2009. However, surface pCO_2 showed a clear increase trend during 1962–2012, especially during 1987–2012. Thus, although MLD variation may lead to increase in surface pCO_2, for example, during 1997–2009 when MLD deepened, it was not the primary factor causing pCO_2 increase over the period 1962–2012.

Biological activity could also affect seawater pCO_2 (e.g., Zhang et al., 2010). We found from 1998 through 2012 there was no significant trend for Chl *a* (Fig. 6d). Model studies also indicated that there were no significant changes in net primary production, particle export production and export efficiency from 1960 to 2006 in this region (Laufkötter et al., 2013). Thus, it revealed that biological activity was not the main factor leading to pCO_2 rise.

In all, surface ocean warming (SST increase) partially contributed to springtime sea surface pCO_2 increase on interannual timescales, while the effects of salinity, MLD, and biological activity were not significant.

3.2.2 Influence of ocean circulation

The increase of the EIO pCO_2 with time may be primarily due to the transport of carbon accumulated in the CO_2 sink region (to the atmosphere) towards the CO_2 source region on a basin scale via ocean circulation. We know that the region between 15° S and 50° S in the Indian Ocean, a major subduction zone of the Indian Ocean (Schott et al., 2009), is a significant sink of atmospheric CO_2 (Fig. 1a, Takahashi et al., 2009; Valsala et al., 2012) and, therefore, anthropogenic CO_2 will be accumulated in this region. For example, it was reported that the inventories of anthropogenic CO_2 were largest in this zone in the Indian Ocean (Sabine et al., 2004), and the oceanic increase in carbon storage roughly kept pace with atmospheric CO_2 increase (Sabine et al., 1999).

On the other hand, ocean circulations (e.g., a shallow meridional overturning circulation) in the Indian Ocean allow the carbon accumulated in the CO_2 sink region to be transported towards the equatorial Indian Ocean (Fig. 1, Schott et al., 2002, 2009; Valsala et al., 2012). For instance, subducted water masses first move westward in the South Equatorial Current (SEC), which splits into the Northeast and the Southeast Madagascar Currents, then part of the subducted water masses merge into the East African Coast Current (EACC), and finally a fraction of the northern SEC/EACC inflow returns eastward just south of the equator during the winter monsoon with the South Equatorial Countercurrent (SECC), which exists year round, except that it is subsurface during the summer monsoon (Fig. 1, Schott and McCreary, 2001; Schott et al., 2009 and references therein). At this time, at the eastern end of the SECC, the South Java Current (SJC, Fig. 1) flows southeastward (Schott and McCreary, 2001). In addition, the strong eastward Wyrtki jets (Wyrtki, 1973; Schott and McCreary, 2001) in the surface layer and the eastward Equatorial Undercurrent (Knauss and Taft, 1964) in the subsurface layer may also play an important role in transporting waters eastward (Xuan et al., 2012). Thus, the southern subtropical Indian Ocean acted as a window for carbon uptake (Valsala et al., 2012) and part of the absorbed CO_2 could be ultimately transported to the northern Indian Ocean including the equatorial belt. Similar mechanism was also proposed in the equatorial Pacific by Feely et al. (1999), who pointed out that the entrained subtropical water was injected into the upwelled water at the equator.

Nevertheless, the pathways of ocean circulations are very complicated, and there must be other ways to increase pCO_2 in the equatorial Indian Ocean. For instance, the Red Sea–Persian Gulf Intermediate Water formed in the northwestern Indian Ocean carry anthropogenic CO_2 signals and spread equatorward (Sabine et al., 2004; Alvarez et al., 2009 and references therein), which also contributes to the increase of equatorial waters pCO_2. Thus, further studies on carbon transport should be conducted in the Indian Ocean in the future. Even so, we speculate that the CO_2 sink region to the atmosphere may be a window for CO_2 uptake (e.g., Valsala et al., 2012), and the mixing between waters in the CO_2 sink region and the CO_2 source region via large

Observed pCO_2 increase in the equatorial Indian Ocean

L. Xue et al.

Printer-friendly Version

Interactive Discussion

scales ocean circulation may be driving the pCO_2 trend in the global ocean to tend towards that in the atmosphere (Fay and McKinley, 2013). Thus, signal of increasing atmospheric CO_2 was transmitted to the global ocean this way.

3.3 Implications and impacts of surface pCO_2 increase

Increase in surface pCO_2 will impact oceanic CO_2 uptake. In the EIO, the mean pCO_2 increase rate during spring in the ocean ($\sim 1.7\,\mathrm{\mu atm\,yr^{-1}}$) is larger than that in the atmosphere measured at Mauna Loa, Hawaii ($1.41\,\mathrm{\mu atm\,yr^{-1}}$, Fig. 4a). It indicates that the driving force of CO_2 air–sea exchange ($\Delta pCO_2 = pCO_{2\,\mathrm{sea}} - pCO_{2\,\mathrm{air}}$) became larger than before. Thus, more and more CO_2 in this CO_2 source region would be released from the ocean to the atmosphere, which may cause the decrease of global oceanic carbon sink, if the gas transfer velocity keeps constant. Also a decrease in oceanic carbon sink has been observed in other oceans such as in the North Atlantic (Lefvre et al., 2004; Schuster et al., 2009) due to the faster increase of oceanic pCO_2 than atmospheric pCO_2.

In addition, oceanic pCO_2 increase may alter the speciation of seawater carbon chemistry, probably exerting negative effects on marine organisms and ecosystems (Doney et al., 2009). Oceanic pCO_2 rise means the increase in seawater CO_2 and HCO_3^- concentrations, and decrease in CO_3^{2-} and pH levels (i.e., OA). Given that in surface waters of most oceans the $CaCO_3$ saturation state is larger than 1 and $CaCO_3$ dissolution yet does not begin (Feely et al., 2004), TA at the surface may not change due to $CaCO_3$ dissolution (note that CO_2 air–sea exchange does not change TA). Thus, we can assume that TA, salinity and temperature keep constant during the period 1962–2013, and estimate pH (on NBS scales) and aragonite saturation state (Ω_{arg}) from surface pCO_2, TA, temperature and salinity employing CO2sys (Lewis and Wallace, 1998) and adopting the CO_2 system coefficients of Mehrbach et al. (1973) as refitted by Dickson and Millero (1987). In fact, temperature rise and salinity decrease have happened as described in Sect. 3.2.1. They both will lower pH, since temperature

Full Screen / Esc

Printer-friendly Version

Interactive Discussion

rise will raise the concentration of hydrogen ion, and salinity decline will decrease TA. If we use the mean surface TA ($2243 \, \mu\text{mol} \, \text{kg}^{-1}$) estimated by Lee et al. (2006), SSS (34.08), SST (29.60 °C) and mean surface $npCO_2$ in April 1963 and May 2012, surface pH at 25.0 °C in the EIO would decrease from 8.33 in April 1963 to 8.26 in May 2012

5 (mean surface pH in the 2012 MOMSEI cruise was 8.23 ± 0.02), and correspondingly aragonite saturation state (Ω_{arg}) would drop from 4.4 to 3.9. Reduction in pH (0.07 pH units) during the past 50 yr (1963–2012) in the EIO is surprising, considering that the average surface ocean pH has just declined by about 0.1 units since the 1700s due to the absorption of anthropogenic CO_2 (Raven et al., 2005).

10 Noticeably, sea surface pCO_2 increase has been observed in various oceanic zones, some of which serve as CO_2 sinks and some as CO_2 sources to the atmosphere (Table 3). It seems that ocean pCO_2 is rising on a global scale due to the forcing of rising atmospheric CO_2 and global warming (Fay and McKinley, 2013). It also demonstrated that OA may have taken place in the global ocean, not just limited to the CO_2 sink

15 region.

4 Summary and conclusions

Results showed that sea surface pCO_2 during spring in the EIO significantly increased from 1962 to 2012, with a mean rate of $\sim 1.7 \, \mu\text{atm} \, \text{yr}^{-1}$. Assessing the trend of surface pCO_2 in the study area is full of challenge due to lack of continuous data, and more

20 observations with good temporal and spatial resolutions are needed in the future. However, this study not only provides direct evidence for OA in the Indian Ocean, but also implies that changes in other marine biogeochemical processes may have taken place in the Indian Ocean since the IIOE conducted during 1960–1965.

Given that the EIO during the study period was almost always a CO_2 source to the

25 atmosphere, it was obvious that the observed increase of springtime sea surface pCO_2 with time in this region was not due to the local uptake of CO_2 via air–sea exchange, although quickly increasing atmospheric CO_2 had the potential to increase seawater

pCO_2. We found surface ocean warming partially contributed to sea surface pCO_2 increase, whereas the effects of salinity, mixed layer depth, and biological activity were not significant. The pCO_2 increase in the equatorial waters was probably due to the transport of carbon accumulated in the CO_2 sink region (to the atmosphere) towards the CO_2 source region on a basin scale via ocean circulation. Additionally, our study showed that more and more release of CO_2 from the ocean to the atmosphere and big pH reduction (0.07 pH units) in the past 50 yr (from 1963 to 2012) may have occurred in the EIO. In conjunction with the studies conducted in various oceanic zones about interannual variations in sea surface pCO_2, it seems that sea surface pCO_2 increase on interannual timescales occurs in both CO_2 source and sink regions, and possibly that ocean pCO_2 is rising on a global scale due to the forcing of rising atmospheric CO_2 level and global warming (Fay and McKinley, 2013). It also demonstrated that OA may have taken place in the global ocean, not just limited to the CO_2 sink region.

References

Álvarez, M., Lo Monaco, C., Tanhua, T., Yool, A., Oschlies, A., Bullister, J. L., Goyet, C., Metzl, N., Touratier, F., McDonagh, E., and Bryden, H. L.: Estimating the storage of anthropogenic carbon in the subtropical Indian Ocean: a comparison of five different approaches, Biogeosciences, 6, 681–703, doi:10.5194/bg-6-681-2009, 2009.

Bates, N. R.: Interannual variability of the oceanic CO_2 sink in the subtropical gyre of the North Atlantic Ocean over the last 2 decades, J. Geophys. Res., 112, C09013, doi:10.1029/2006JC003759, 2007.

Bates, N. R., Pequignet, A. C., and Sabine, C. L.: Ocean carbon cycling in the Indian Ocean: 1. Spatiotemporal variability of inorganic carbon and air–sea CO_2 gas exchange, Global Biogeochem. Cy., 20, GB3020, doi:10.1029/2005GB002491, 2006.

Denman, K. L., Brasseur, G., Chidthaisong, A., Ciais, P., Cox, P. M., Dickinson, R. E., Hauglustaine, D., Heinze, C., Holland, E., Jacob, D., Lohmann, U., Ramachandran, S., Da Silva Dias, P. L., Wofsy, S. C., and Zhang, X.: Couplings between changes in the climate system and biogeochemistry, in: Climate Change 2007: The Physical Science Basis, Contribution of Working Group I to the Fourth Assessment Report of the Intergovernmental Panel on Climate Change, edited by: Solomon, S., Qin, D., Manning, M., Chen, Z., Marquis, M., Averyt, K. B., Tignor, M., and Miller, H. L., Cambridge Press, Cambridge, 541–584, 2007.

Dickson, A. G. and Millero, F. J.: A comparison of the equilibrium constants for the dissociation of carbonic acid in seawater media, Deep-Sea Res., 34, 1733–1743, 1987.

Doney, S. C., Fabry, V. J., Feely, R. A., and Kleypas, J. A.: Ocean acidification: the other CO_2 problem, Annual Review of Marine Science, 1, 169–192, 2009.

Dumousseaud, C., Achterberg, E. P., Tyrrell, T., Charalampopoulou, A., Schuster, U., Hartman, M., and Hydes, D. J.: Contrasting effects of temperature and winter mixing on the seasonal and inter-annual variability of the carbonate system in the Northeast Atlantic Ocean, Biogeosciences, 7, 1481–1492, doi:10.5194/bg-7-1481-2010, 2010.

Fay, A. R. and McKinley, G. A.: Global trends in surface ocean pCO_2 from in situ data, Global Biogeochem. Cy., 27, 1–17, doi:10.1002/gbc.20051, 2013.

Feely, R. A., Wanninkhof, R., Takahashi, T., and Tans, P.: Influence of El Nino on the equatorial Pacific contribution to atmospheric CO_2 accumulation, Nature, 398, 597–601, 1999.

Feely, R. A., Sabine, C. L., Lee, K., Berelson, W., Kleypas, J., Fabry, V. J., and Millero, F. J.: Impact of anthropogenic CO_2 on the $CaCO_3$ system in the oceans, Science, 305, 362–366, 2004.

Ishii, M., Inoue, H. Y., Midorikawa, T., Saito, S., Tokieda, T., Sasano, D., Nakadate, A., Nemoto, K., Metzl, N., Wong, C. S., and Feely, R. A.: Spatial variability and decadal trend of the oceanic CO_2 in the western equatorial Pacific warm/fresh water, Deep-Sea Res. Pt. II, 56, 591–606, 2009.

Jiang, L. Q., Cai, W.-J., Wanninkhof, R., Wang, Y., and Lüger, H.: Air–sea CO_2 fluxes on the US South Atlantic Bight: spatial and seasonal variability, J. Geophys. Res., 113, C07019, doi:10.1029/2007JC004366, 2008.

Keerthi, M. G., Lengaigne, M., Vialard, J., de Boyer Montégut, C., and Muraleedharan, P. M.: Interannual variability of the Tropical Indian Ocean mixed layer depth, Ocean Dynam., 40, 743–759, 2013.

Title Page

Abstract | Introduction

Conclusions | References

Tables | Figures

◄ | ►

◄ | ►

Back | Close

Full Screen / Esc

Printer-friendly Version

Interactive Discussion

Knauss, J. A. and Taft, B. A.: Equatorial undercurrent of the Indian Ocean, Science, 143, 354–356, 1964.

Laufkötter, C., Vogt, M., and Gruber, N.: Long-term trends in ocean plankton production and particle export between 1960–2006, Biogeosciences, 10, 7373–7393, doi:10.5194/bg-10-7373-2013, 2013.

Lee, K., Tong, L. T., Millero, F. J., Sabine, C. L., Dickson, A. G., Goyet, C., Park, G., Wanninkhof, R., Feely, R. A., and Key, R. M.: Global relationships of total alkalinity with salinity and temperature in surface waters of the world's oceans, Geophys. Res. Lett., 33, L19605, doi:10.1029/2006GL027207, 2006.

Lefèvre, N., Watson, A. J., Olsen, A., Ríos, A. F., Pérez, F. F., and Johannessen, T.: A decrease in the sink for atmospheric CO_2 in the North Atlantic, Geophys. Res. Lett., 31, L07306, doi:10.1029/2003GL018957, 2004.

Lenton, A., Metzl, N., Takahashi, T., Kuchinke, M., Matear, R. J., Roy, T., Sutherland, S. C., Sweeney, C., and Tilbrook, B.: The observed evolution of oceanic pCO_2 and its drivers over the last two decades, Global Biogeochem. Cy., 26, GB2021, doi:10.1029/2011GB004095, 2012.

Lewis, E. and Wallace, D. W. R.: Program developed for CO_2 systems calculations, ORNL/CDIAC 105, Carbon Dioxide Information Analysis Center, Oak Ridge National Laboratory US Department of Energy, Oak Ridge, Tennessee, 1998.

Mehrbach, C., Culberson, C. H., Hawley, J. E., and Pytkowicz, R. M.: Measurement of the apparent dissociation constants of carbonic acid in seawater at atmospheric pressure, Limnol. Oceanogr., 18, 897–907, 1973.

Metzl, N.: Decadal increase of oceanic carbon dioxide in Southern Indian Ocean surface waters (1991–2007), Deep-Sea Res. Pt. II, 56, 607–619, 2009.

Millero, F. J.: The marine inorganic carbon cycle, Chem. Rev., 107, 308–341, 2007.

Naqvi, S.: Air–sea interactions and exchanges, in: Report of the Indian Ocean Synthesis Group on the Arabian Sea Process Study, edited by: Watts, L., Burkill, P., and Smith, S., JGOFS International Project Office, University of Bergen, Norway, 13–23, 2002.

Omar, A. M. and Olsen, A.: Reconstructing the time history of the air–sea CO_2 disequilibrium and its rate of change in the eastern subpolar North Atlantic, 1972–1989, Geophys. Res. Lett., 33, L04602, doi:10.1029/2005GL025425, 2006.

Oudot, C., Ternon, J., and Lecomte, J.: Measurements of atmospheric and oceanic CO_2 in the tropical Atlantic: 10 years after the 1982–1984 FOCAL cruises, Tellus B, 47, 70–85, 1995.

Park, G. and Wanninkhof, R.: A large increase of the CO_2 sink in the western tropical North Atlantic from 2002 to 2009, J. Geophys. Res., 117, C08029, doi:10.1029/2011JC007803, 2012.

Raven, J., Caldeira, K., Elderfield, H., Hoegh-Guldberg, O., Liss, P., Riebesell, U., Shepherd, J., Turley, C., and Watson, A.: Ocean Acidification Due to Increasing Atmospheric Carbon Dioxide, The Royal Society, London, 1–60, 2005.

Sabine, C. L. and Key, R. M.: Controls on $f CO_2$ in the South Pacific, Mar. Chem., 60, 95–110, 1998.

Sabine, C. L., Key, R. M., Johnson, K. M., Millero, F. J., Poisson, A., Sarmiento, J. L., Wallace, D. W. R., and Winn, C. D.: Anthropogenic CO_2 inventory of the Indian Ocean, Global Biogeochem. Cy., 13, 179–198, 1999.

Sabine, C. L., Key, R. M., Feely, R. A., and Greeley, D.: Inorganic carbon in the Indian Ocean: distribution and dissolution processes, Global Biogeochem. Cy., 16, 1067, doi:10.1029/2002GB001869, 2002.

Sabine, C. L., Feely, R. A., Gruber, N., Key, R. M., Lee, K., Bullister, J. L., Wanninkhof, R., Wong, C. S., Wallace, D. W. R., Tilbrook, B., Millero, F. J., Peng, T. H., Kozyr, A., Ono, T., and Rios, A. F.: The oceanic sink for anthropogenic CO_2, Science, 305, 367–371, 2004.

Sabine, C. L., Hankin, S., Koyuk, H., Bakker, D. C. E., Pfeil, B., Olsen, A., Metzl, N., Kozyr, A., Fassbender, A., Manke, A., Malczyk, J., Akl, J., Alin, S. R., Bellerby, R. G. J., Borges, A., Boutin, J., Brown, P. J., Cai, W.-J., Chavez, F. P., Chen, A., Cosca, C., Feely, R. A., González-Dávila, M., Goyet, C., Hardman-Mountford, N., Heinze, C., Hoppema, M., Hunt, C. W., Hydes, D., Ishii, M., Johannessen, T., Key, R. M., Körtzinger, A., Landschützer, P., Lauvset, S. K., Lefèvre, N., Lenton, A., Lourantou, A., Merlivat, L., Midorikawa, T., Mintrop, L., Miyazaki, C., Murata, A., Nakadate, A., Nakano, Y., Nakaoka, S., Nojiri, Y., Omar, A. M., Padin, X. A., Park, G.-H., Paterson, K., Perez, F. F., Pierrot, D., Poisson, A., Ríos, A. F., Salisbury, J., Santana-Casiano, J. M., Sarma, V. V. S. S., Schlitzer, R., Schneider, B., Schuster, U., Sieger, R., Skjelvan, I., Steinhoff, T., Suzuki, T., Takahashi, T., Tedesco, K., Telszewski, M., Thomas, H., Tilbrook, B., Vandemark, D., Veness, T., Watson, A. J., Weiss, R., Wong, C. S., and Yoshikawa-Inoue, H.: Surface Ocean CO_2 Atlas (SOCAT) gridded data products, Earth Syst. Sci. Data, 5, 145–153, doi:10.5194/essd-5-145-2013, 2013.

Saderne, V., Fietzek, P., and Herman, P. M. J.: Extreme variations of pCO_2 and pH in a macrophyte meadow of the Baltic Sea in summer: evidence of the effect of photosynthesis and local upwelling, PLoS ONE, 8, e62689, doi:10.1371/journal.pone.0062689, 2013.

Sardessai, S., Maya, M. V., Shetye, S., PrasannaKumar, S., Fernandes, V., Paul, J., and Ra-
maiah, N.: Environmental controls on the seasonal carbon dioxide fluxes in the northeastern
Indian Ocean, Indian J. Mar. Sci., 39, 192–200, 2010.

Sarma, V. V. S. S., Lenton, A., Law, R. M., Metzl, N., Patra, P. K., Doney, S., Lima, I. D., Dlugo-
kencky, E., Ramonet, M., and Valsala, V.: Sea–air CO_2 fluxes in the Indian Ocean between
1990 and 2009, Biogeosciences, 10, 7035–7052, doi:10.5194/bg-10-7035-2013, 2013.

Schott, F. A. and McCreary, J. P.: The monsoon circulation of the Indian Ocean, Prog.
Oceanogr., 51, 1–123, 2001.

Schott, F. A., Dengler, M., and Schoenefeldt, R.: The shallow overturning circulation of the
Indian Ocean, Prog. Oceanogr., 53, 57–103, 2002.

Schott, F. A., Xie, S., and McCreary Jr., J. P.: Indian Ocean circulation and climate variability,
Rev. Geophys., 47, RG1002, doi:10.1029/2007RG000245, 2009.

Schuster, U., Watson, A. J., Bates, N. R., Corbiere, A., Gonzalez-Davila, M., Metzl, N., Pier-
rot, D., and Santana-Casiano, M.: Trends in North Atlantic sea-surface $f CO_2$ from 1990 to
2006, Deep-Sea Res. Pt. II, 56, 620–629, 2009.

Smith, T. M., Reynolds, R. W., Peterson, T. C., and Lawrimore, J.: Improvements to NOAA's his-
torical merged land-ocean surface temperature analysis (1880–2006), J. Climate, 21, 2283–
2296, 2008.

Subrahmanyam, B., Murty, V. S. N., and Heffner, D. M.: Sea surface salinity variability in the
tropical Indian Ocean, Remote Sens. Environ., 115, 944–956, 2011.

Tans, P. and Keeling, R.: Trends in atmospheric carbon dioxide, NOAA/ESRL, available at:
www.esrl.noaa.gov/gmd/ccgg/trends/ (last access: 3 December 2013), 2013.

Takahashi, T., Olafsson, J., Goddard, J. G., Chipman, D. W., and Sutherland, S. C.: Seasonal
variation of CO_2 and nutrients in the high-latitude surface oceans: a comparative study,
Global Biogeochem. Cy., 7, 843–878, 1993.

Takahashi, T., Sutherland, S. C., Feely, R. A., and Cosca, C. E.: Decadal variation of the surface
water pCO_2 in the western and central equatorial Pacific, Science, 302, 852–856, 2003.

Takahashi, T., Sutherland, S. C., Feely, R. A., and Wanninkhof, R.: Decadal change of the
surface water pCO_2 in the North Pacific: a synthesis of 35 years of observations, J. Geophys.
Res., 111, C07S05, doi:10.1029/2005JC003074, 2006.

Takahashi, T., Sutherland, S. C., Wanninkhof, R., Sweeney, C., Feely, R. A., Chipman, D. W.,
Hales, B., Friederich, G., Chavez, F., Sabine, C., Watson, A., Bakker, D. C. E., Schuster, U.,
Metzl, N., Yoshikawa-Inoue, H., Ishii, M., Midorikawa, T., Nojiri, Y., Körtzinger, A., Stein-

Title Page

Abstract | Introduction

Conclusions | References

Tables | Figures

|◄ | ►|

◄ | ►

Back | Close

Full Screen / Esc

Printer-friendly Version

Interactive Discussion

hoff, T., Hoppema, M., Olafsson, J., Arnarson, T. S., Tilbrook, B., Johannessen, T., Olsen, A., Bellerby, R., Wong, C. S., Delille, B., Bates, N. R., and de Baar, H. J. W.: Climatological mean and decadal change in surface ocean pCO_2, and net sea–air CO_2 flux over the global oceans, Deep-Sea Res. Pt. II, 56, 554–577, 2009.

Takahashi, T., Sutherland, S. C., and Kozyr, A.: Global ocean surface water partial pressure of CO_2 database: measurements performed during 1957–2012 (version 2012), ORNL/ORNL/CDIAC-160, NDP-088 (V2012), Carbon Dioxide Information Analysis Center, Oak Ridge National Laboratory, US Department of Energy, Oak Ridge, Tennessee, doi:10.3334/CDIAC/OTG.NDP088(V2012), 2013.

Valsala, V. and Maksyutov, S.: Interannual variability of the air–sea CO_2 flux in the north Indian Ocean, Ocean Dynam., 63, 1–14, 2013.

Valsala, V., Maksyutov, S., and Murtugudde, R.: A window for carbon uptake in the southern subtropical Indian Ocean, Geophys. Res. Lett., 39, L17605, doi:10.1029/2012GL052857, 2012.

Wyrtki, K.: An equatorial jet in the Indian Ocean, Science, 181, 262–264, 1973.

Xuan, L. L., Qiu, Y., Xu, J., and He, Y.: Hydrography and circulation in the eastern tropical Indian Ocean during April-May 2011, Atmospheric and Oceanic Science Letters, 5, 284–289, 2012.

Xue, L., Xue, M., Zhang, L., Sun, T., Guo, Z., and Wang, J.: Surface partial pressure of CO_2 and air–sea exchange in the northern Yellow Sea, J. Marine Syst., 105–108, 194–206, 2012.

Zhang, L., Xue, L., Song, M., and Jiang, C.: Distribution of the surface partial pressure of CO_2 in the southern Yellow Sea and its controls, Cont. Shelf Res., 30, 293–304, 2010.

Title Page

Abstract | Introduction

Conclusions | References

Tables | Figures

◄ | ►

◄ | ►

Back | Close

Full Screen / Esc

Printer-friendly Version

Interactive Discussion

Table 1. Summary of cruise information and data used for this study. Surface temperature, surface pCO_2, and pCO_2 normalized to a constant temperature of 29.60 °C (npCO_2), the mean temperature of all data, are reported in the form of mean ± standard deviation.

Cruise name	Observation period[a]	Ship/ experiment	Surface temperature	Surface pCO_2	Surface npCO_2	Data number
LUSIAD_62	30 Jun, 2–3 Jul 1962	R/V *Argo*	29.24 ± 0.21	304 ± 2	308 ± 2	39
LUSIAD_63	8–26 Apr 1963	R/V *Argo*	29.78 ± 0.43	308 ± 8	306 ± 7	230
SAGA_II_Leg_2	30 Jun–2 Jul 1987	R/V *A. Korolev* SAGA II	29.06 ± 0.23	360 ± 9	368 ± 9	49
R.F. Weiss Surface Data Files 42–63	10–17 Feb 1995	R/V *Knorr* Weiss Data	29.54 ± 0.28	352 ± 4	353 ± 5	367
IO95leg	31 Oct–1 Nov 1995	R/V *M. Baldrige* IO95	29.06 ± 0.13	362 ± 2	370 ± 2	203
JASMINE1999_2	4–6, 28–31 May 1999	R/V *Ron Brown* 1999	29.24 ± 0.32	373 ± 8	379 ± 7	814
I09N_Underway_pCO_2	9–16 Apr 2007	CLIVAR Repeat Sections	29.81 ± 0.39	385 ± 6	382 ± 8	1411
MOMSEI	1–9 May 2012	R/V *Madidihang* 03	29.98 ± 0.26	387 ± 7	381 ± 7	471

[a] The observed period in this table refers to the period when the data used in this study were collected. And data before 2012 are integrated by Takahashi et al. (2013) (i.e., http://cdiac.ornl.gov/ftp/oceans/LDEO_Database/Version_2012/, LDEO_Database_V2012).

Table 2. Sources of data used in this study.

Parameter	Source
Sea surface temperature[a]	Extended Reconstructed Sea Surface Temperature (ERSST.v3b) with a spatial revolution of 1° × 1° (http://www.ncdc.noaa.gov/ersst/)
Mixed layer depth[b]	IFREMER/LOS Mixed Layer Depth Climatology website with a spatial resolution of 2° × 2° (www.ifremer.fr/cerweb/deboyer/mld)
Chlorophyll a[c]	SeaWiFS with a spatial resolution of 0.1° × 0.1°, (http://las.pfeg.noaa.gov/oceanWatch/oceanwatch.php)
Sea surface pCO_2[d]	LDEO_Database_V2012 (Takahashi et al., 2013) (http://cdiac.ornl.gov/ftp/oceans/LDEO_Database/Version_2012/)
Atmospheric CO_2[e]	Mauna Loa CO_2 monthly mean data (http://www.esrl.noaa.gov/gmd/ccgg/trends/mlo.html)

[a] ERSST.v3b is the most recent version, from US National Oceanic and Atmospheric Administration, National Climatic Data Center. Details on ERSST.v3 are described in Smith et al. (2008). Monthly mean data in the study area (5° N to 5° S along 90° E and 95° E) during April/May from 1962–2012 are selected.

[b] This mixed layer depth is in fact a temperature-mixed layer depth, or isothermal layer depth. Mixed layer depths are computed as the depth with a 0.2 °C absolute temperature difference from 10 m temperature (Keerthi et al., 2013). Monthly mixed layer depth data during April from 1969 to 2009 in the study area are used.

[c] Chlorophyll a data during April/May from 1998 to 2012 are used.

[d] See specific cruise information in Table 1.

[e] Atmospheric CO_2 data were measured as the mole fraction in dry air on Mauna Loa, Hawaii, the longest record of direct measurements of CO_2 in the atmosphere. Monthly mean values during 1962–2012 were used.

Table 3. Sea surface pCO_2 trend observed in various regions of the ocean.

Region	Period	pCO_2 growth rate ($\mu atm\,yr^{-1}$)	sink/source[a]	Reference
Eastern subpolar Atlantic (32–10° W, 50° N–64° N)	1972–1989	2.3(±0.8)	sink	Omar and Olsen (2006)
Subtropical North Atlantic near Bermuda	1983–2003	1.7(±0.3)	sink	Bates (2007)
Western tropical North Atlantic	2002–2009	1.01–1.11	sink	Park and Wanninkhof (2012)
Eastern Eq. Atlantic	1982–1992[b]	2.5–2.8	source	Oudot et al. (1995)
Subarctic Western North Pacific	1995–2003	1.6(±1.7)	sink	Lenton et al. (2012)
Western Subtropical North Pacific	1995–2005	1.8(±0.6)	sink	Lenton et al. (2012)
Eq. Pacific (Niño 3.4 and Warm Pool regions included)	1990–2004	1.8–2.3	source	Takahashi et al. (2006)
East Eq. Indian Ocean (90–100° E, 5° S–5° N, Spring)	1963–2012	1.7–1.8	source	This study
Southwestern Indian Ocean (30–90° E, 50–55° S, Summer)	1991–2007	2.4(±0.2)	sink	Metzl (2009)
Indian and Pacific sectors of Southern Ocean	1995–2008	2.2(±0.2)	sink	Lenton et al. (2012)

[a] Sink means that the ocean absorbs atmospheric CO_2 while source indicates that the ocean releases CO_2 to the atmosphere.
[b] The growth rate here refers to the mean difference between 1982 and 1992.
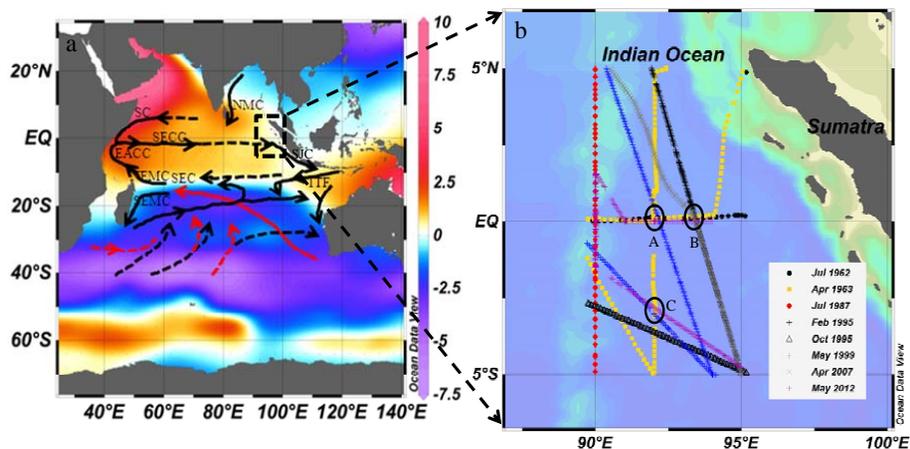
Fig. 1. Study site. **(a)** shows the relative location of the study site (within the dashed frame) in the Indian Ocean, and annual air–sea CO_2 fluxes ($mol\,C\,m^{-2}\,yr^{-1}$, colored) estimated by Taka-hashi et al. (2009) as well as schematic representations of ocean currents during the winter monsoon redrawn from Schott et al. (2009) as an example. The currents shown in this map include the South Equatorial Current (SEC), South Equatorial Countercurrent (SECC), Northeast and Southeast Madagascar Current (NEMC and SEMC), East African Coastal Current (EACC), Somali Current (SC), Indonesian Throughflow (ITF), South Java Current (SJC), the Northeast Monsoon Current (NMC) during the winter monsoon, and so on. Also the subsurface return flow for the supergyre is shown in red. **(b)** shows the study site, the East Equatorial Indian Ocean (EIO, 5° N–5° S, 90–95° E). The lines show all cruise tracks for surface CO_2 partial pressure (pCO_2) measurement during 1962–2012 in the EIO. And the black circle A (0, 92(±0.3)° E), B (0, 93.4(±0.3)° E), and C (2.9(±0.3)° S, 92° E) present the locations that several cruises almost repeatedly occupied.
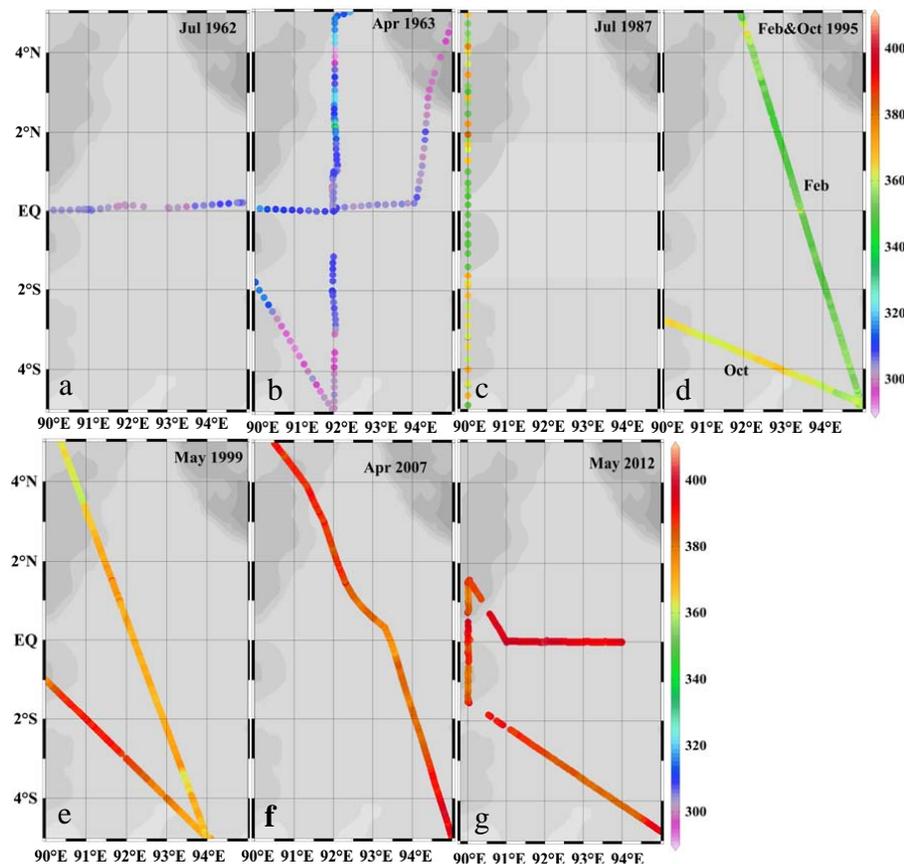
Fig. 2. Sea surface CO$_2$ partial pressure (*p*CO$_2$) observed in July 1962 **(a)**, April 1963 **(b)**, July 1987 **(c)**, February and October 1995 **(d)**, May 1999 **(e)**, April 2007 **(f)**, and May 2012 **(g)** in the EIO.
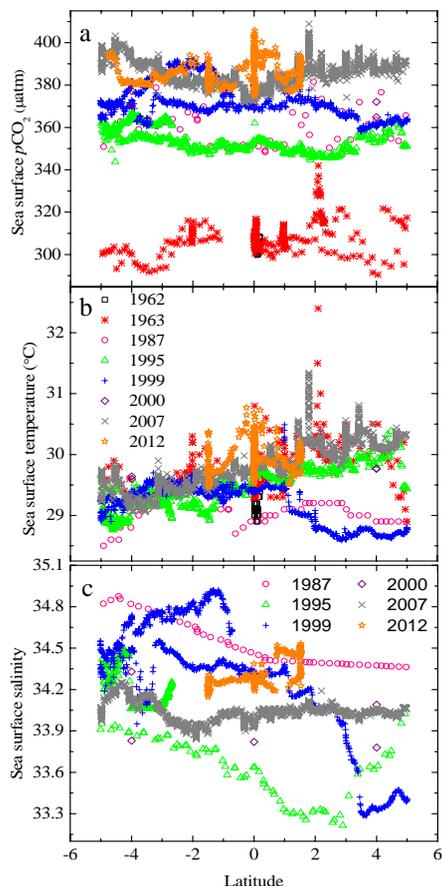
Fig. 3. Latitudinal distribution of sea surface pCO_2, temperature and salinity measured in the study area during 1962–2012. Data in 2000 are from Takahashi et al. (2009)'s grid data. Meanings of symbols in **(a)** are the same as those in **(b)**.

546
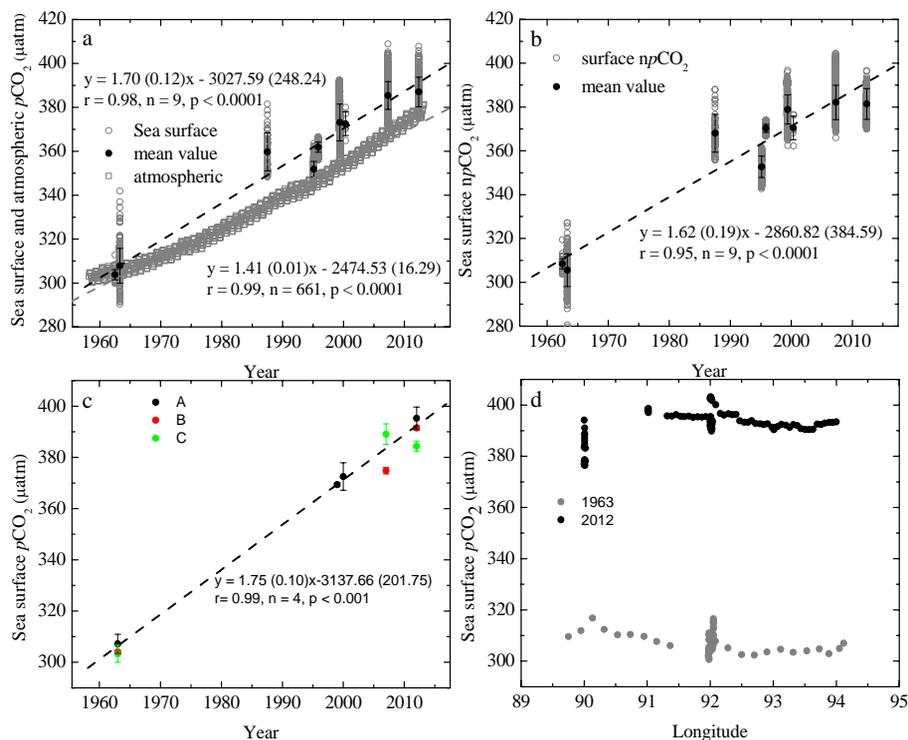
Fig. 4. Temporal change in in-situ sea surface pCO_2 (gray circle) and atmospheric pCO_2 (gray square) measured at Mauna Loa, Hawaii **(a)**, surface pCO_2 normalized to a constant temperature of 29.60 °C (npCO_2, **b**), in-situ mean surface pCO_2 at typical points (i.e., A, B and C in Fig. 1, **c**), and sea surface pCO_2 along the equator during April 1963 and May 2012 **(d)**. The dashed lines in **(a)** and **(b)** show linear regressions based on mean value of each cruise (solid circle), whereas the dashed line in **(c)** indicates a linear regression based on data from point A.
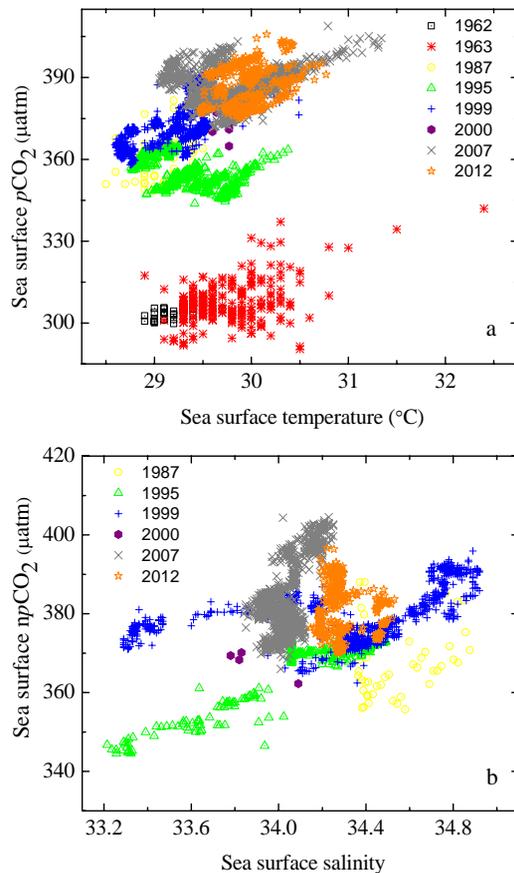
Fig. 5. Scatterplots of surface pCO_2 with temperature **(a)**, and surface pCO_2 normalized to a constant temperature of 29.60 °C (npCO_2) with salinity **(b)** for all in-situ data during 1963–2012.

Title Page

Abstract | Introduction

Conclusions | References

Tables | Figures

|◀ | ▶|

◀ | ▶

Back | Close

Full Screen / Esc

Printer-friendly Version

Interactive Discussion
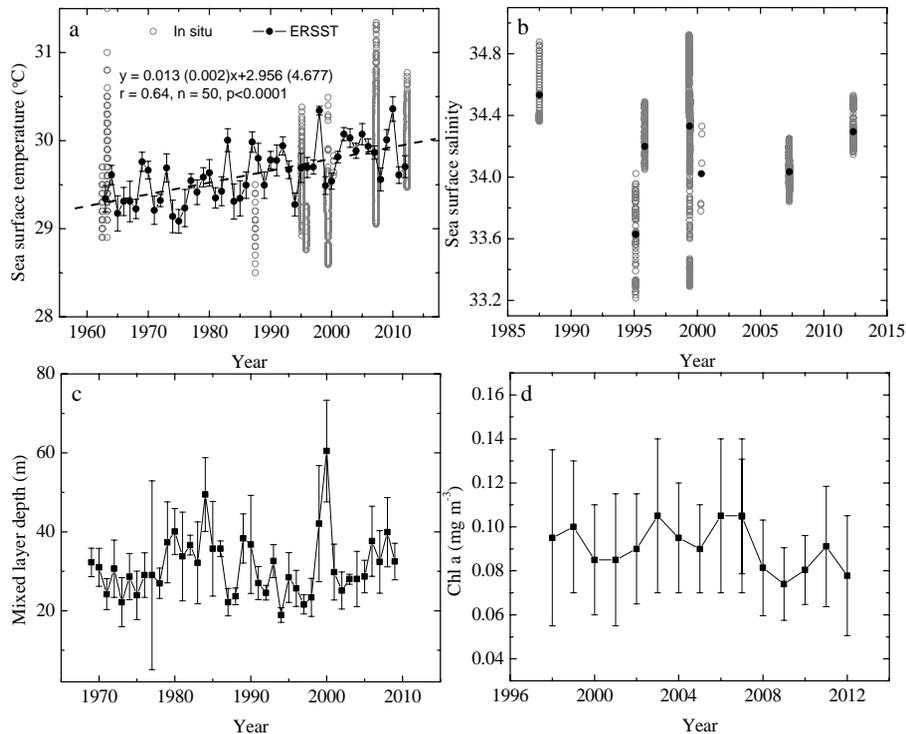
Fig. 6. Temporal change in sea surface temperature **(a)**, salinity **(b)**, mixed layer depth **(c)**, and chlorophyll *a* (Chl *a*, **d**). In **(a)**, gray circles indicate in situ data and solid circles extended reconstructed sea surface temperature, ERSST; in **(b)**, gray circles indicate in situ data and solid circles mean value of each cruise; in **(c)** and **(b)**, squares show the mean value, and bars show the standard deviation. See Table 2 for more details.

Title Page

Abstract | Introduction

Conclusions | References

Tables | Figures

◀◀ | ▶▶

◀ | ▶

Back | Close

Full Screen / Esc

Printer-friendly Version

Interactive Discussion